ATLAS Internal Note
MUON-NO-109
1st March 1996

X-RAY TOMOGRAPHY. TEST OF NEW SETUP AND MEASUREMENT OF 4x8 DRIFT TUBE PROTOTYPE.

A.Borisov, V.Goryatchev, R.Fakhroutdinov, A.Kozhin,
A.Vovenko, S.Zimin.

Institute for High Energy Physics
Protvino, 142284, Moscow region, Russia

1 Introduction

In our previous work/1,2/ it was shown that a X-ray pulser can be used to measure a wire position inside drift tube. The similar approach for wire position measurement based on JINR group work /3/ was developed at CERN utilizing continuous mode of X-ray source. X-ray pulser requires less power consumption and in our case X-ray power is about 3 or more order of magnitude less as compare to CERN tomography X-ray setup. Pulsed mode is well matched to drift tube DAQ with trigger from the X-ray pulser and the drift tubes can be used themselves as detector of X-ray. Moreover triggered mode reduce background and it allowed us to measure 4 tube layers with relatively small anode voltage of X-ray tube.

Now we prepared new more realistic setup with two simultaneous beams. The beam angles were chosen to measure wires inside MDT chamber with dense package of tube.

Goals of this work are test of the setup and measurement of 4x8 drift tube prototype.

2 4x8 drift tube prototype

The prototype consists of 32 Al tubes of 20 cm long with dense package (fig.1). Outer tube diameter is 30 mm, the most of tubes have wall thickness of 0.5 mm. Seven tubes (13-16,18-20) have wall thickness 0.25 mm. Precise element of design is an end plug with outer diameter 30.1±0.002 mm (RMS). Sense wires are made of 50 μm gold-plated tungsten. Tubes are glued together in points of their touching. Length of glue layer is equal to tube one. Width of glue layer is about of 1-2 mm. The gluing of the prototype was done in a cassette. Mechanical tolerances of the cassette is 20 μm. After hardening of the glue the cassette was removed.

The prototype has been tested at M2 test beam area of ATLAS MDT at CERN from 5 August to 8 September of 1995. Preliminary analysis gives residuals distribution with sigma about 69 μm and about of zero offset for 8 point tracks for HV corresponding to streamer mode. This is an indication of good mechanical quality of the prototype.

3 Setup

Brief description of the X-ray pulser is given in /4/. It can give X-ray pulses with minimal duration of 15 ns. Frequency and maximal duration of the pulses are limited only by the heating of tube. In principle it can work in continuous mode with water cooling. An admitted anode voltage is 45 kV. The most of results which will be given below were obtained with X-ray tube anode voltage 23 kV, pulse duration 10 μs and frequency 100 Hz.

In fig. 1 cross-section of our setup is shown schematically. Two X-ray tubes are closed in a metallic box. They give two beams which have inclination angles with respect to horizontal direction about 60.5° and 120.5° accordingly for beam 1 and 2. Such angles were chosen specially for measurement of wires inside MDT chambers with dense package of tubes. There is some small deviation of the angles from exact values of 60° and 120° to

prevent overlap of measured wires. For our setup to measure one tube "road", e.g. wires in tubes 1,5,10,14 (fig.1) by beam 2, it is need to scan range about of 1.5-2mm.

The X-ray source spot is $75^{+75}\mu$m and divergency is about 10^{o}, as claimed by a manufacturer. The narrow beam is created by a collimator consisting of two pairs of tungsten rods. The rods diameter is 1 mm and distance between them is 50 μm for the down pair. The distance between the up rods of the collimator is 20 μm for beam 2 and 30-40 μm for beam 1. Width of the collimator along wires (normal to the picture plane) is about 13 mm. The beams were aligned with respect to tested tube wires better than a few mrad.

The box with X-ray tubes is placed on a platform which can be moved on rails attached to a table with ruler. The movement of the platform is driven by handle and its relative position with respect to the table is measured by the ruler with digital output. Maximal length of the ruler is 1 m. The output bin is 5 μm.

4 Test of 4x8 prototype

The 4x8 drift tube prototype is placed above the X-ray pulser. It is attached to the table and is not moved (fig.1).

The tubes were filled with gas mixture Ar and CO_2 at normal pressure with CO_2 fraction 5 or 10%. High voltage of tube was 2.2 kV for 10% CO_2 and 1.7 kV for 5%. Results which will be given below are independent of gas mixture but due to an overload amplifiers at 2.2 kV for 10% CO_2 counting rate for this condition must be scaled about 0.3. We used the same amplifiers and discriminators as at the beam test. TDC of IHEP-JINR neutrino detector was used/5/. We measured a tube counting rate normalized to number of X-ray pulses as a function of beam position. When beam hits a wire a drop of the counting rate appears in next tube layer. The 1st tube which is crossed by beam can detect such drop itself.

4.1 Measurement of wires

Examples of the counting rate dependences taken in ranges near wires are shown in fig.2-6. Tube voltage is 2.2 kV. Fig.2 shows a shadow of the 1st tube wire illuminated by the beam 2. The shadow is seen in tubes 1,5,10,14,19,23. Tube numbers correspond to fig.1. Histogram bars show measured relation of number of tube hits to number of X-ray pulses in percents as a function of relative distance. Number of X-ray pulses was 3000. It was fixed for all measurements. Curves are fits by constant minus gaussian. Mean value of the gaussian was taken as a wire position. Fig.3,4,5 shows the similar results for wire in tube 5,10,14. Wire in the tube 5 is measured by tubes 10,14,19, wire in tube 10 is measured by tubes 14,19 and so on. Fig.6 shows an example for measurement of wire in tube 16 by beam 1.

Error of wire position from fit is less then 1 μm for the lowest tube, 2-6 μm for the 2nd layer, 7-14 μm for the 3d layer and 15-25 μm for the 4th layer for anode voltage of X-ray tube 23 kV.

Measurements like ones shown in fig.2-6 were performed for all prototype wires where it was possible. The under and right side wires were measured by the X-ray beam 1. The

beam 2 can measure the under wires and left side ones. If a wire is measured by two beams we could be able to calculate its X,Y-coordinate. For calibration of setup we used 3 wires in tubes 2,3 and 6 and supposed that distance between them is equal to nominal value of the end plug diameter. When the angles of the X-ray beams and angle of the ruler were found then coordinates of a wire in X,Y-plane were determinated with respect to wire in tube 3 for all wires where measurements by both beams were possible. Deviation of predicted wire position from measured one is given in table 1. For wires with single beam measurement we could be able to calculate the wire displacement in direction normal to the beam. Such results are shown in table 2.

Fig.7 shows histograms of differences between predicted wire position and measured one for X-coordinate (a), for Y-coordinate (b), normal to beam 1 (c) and normal to beam 2 (d). Mean value of the distributions is about zero and RMS deviation is less than 33 μm.

4.2 Tube wall measurement

An example of the counting rate dependences is shown in fig.8 for tube 1,2,5 and 9 when total diameter of tube 1 was scanned. Direction of X-axis corresponds to the beam movement from right to left in fig.1. The counting rate for each tube is proportional to efficiency of X-ray conversion inside tube or length of internal volume of tube crossing by the X-ray beam. It is clearly seen in fig.8. Tube wall position can be detected at least for the 1st tube layer and for some side tubes. In fig.9 part of the counting rate dependences shown in fig.8 is presented with expanded scale. There are several well distinguished regions in fig.9. The 1st one is arranged at left side from arrow 1 in fig.9(a). The X-ray beam crosses tube 9 here. The counting rate for tube 1 is zero and tube 5 detects scattered X-ray arising after absorption of primary X-ray beam in wall of tube 9. It also counts some halo of X-ray beam. Region between arrows 1 and 2 corresponds to X-ray beam inside the wall of tube 5. The outer surface of tube 5 is detected by increasing of its counting rate and by sharp decreasing of tube 9 counting rate. The full beam width is clearly seen (fig.9(c)). The region between arrows 2 and 3 corresponds to the beam inside wall of tube 1. For coordinates after arrow 3 beam entered in gas volume of tube 1. Similar explanation can be done for sharp change of the counting rate at X=232.5 mm in tube 5 and at X=237.1 mm in tube 2 (fig.8). So the wall coordinate can be detected. We could be able to measure outer tube diameter in directions normal to the beams for four tubes of the 1st layer (table 3). Distribution of difference between ideal outer tube diameter equal to 30 mm and measured one is shown in fig.10(a). Mean value is 29 μm and RMS is 50 μm. Distribution of difference between predicted tube wall position and measured one in direction normal to beam is given in fig.10(b). Fig.10(c) shows difference between 15 mm and measured wire-to-wall distance. Distributions in fig.10(b) and 10(c) have mean value about zero and RMS 75 and 60 μm accordingly.

5 Temporal stability

As it is seen from fig.2-6 the measurement of wire position require scan of region about 300-400 μm around wire with step of about 5-10 μm. It is need about 15 minutes

per 1 wire measurement when preliminary estimation of it was done. Hence there is a question about temporal stability of our setup. We tested the question. Two wires in the tube 1 and 4 were measured by X-ray beam 2 and 1 accordingly during period of about 1 month. Switch on/off of X-ray pulser was done every day. Results for wire in the 4th tube measured by the beam 1 are given in fig.11. Fig.11(a) shows the temporal change of the measured wire position, its distribution is shown in fig.11(c). Root mean square deviation is about 33 μm. Large deviation of several points from mean value near 200 hours and 250 hours was caused by measurements done immediately after switch on X-ray pulser when temperature equilibrium was not established. Fig.11(b) shows the temperature dependence of the measured wire coordinate. Temperature was measured in one point of the table. There is a temperature correlation of measured wire coordinate. The measured wire position with temperature cut 20.7°C which corresponds to about 3 hours after switch on X-ray pulser has RMS deviation 16 μm (fig.11(d)). The similar results are given in fig.12 for the wire in tube 1 measured by beam 2. For period of one month RMS deviation of wire position is 26 μm (fig.12(c)). The temperature correlation (fig.12(b)) is seen less clear as compare to the previous wire.

There is long term variation of the measured wires position. But for short period of several days stability at the level of 20 μm can be reached. Temperature variation for measured by the X-ray 1 position of wire in tube 4 is about of 24 μm/°C. Similar value for wire in tube 1 measured by the X-ray 2 is 19 μm/°C. The temperature variation has two contributions. The first one is caused by the table and the prototype support dimensions change due to temperature variation. We should like remember that the table and the prototype support are made of aluminium. Sizes are 1.6x0.75x0.75 m^3. The second contribution is due to the X-ray beam angle change caused by temperature induced deformation of X-ray tube support. The second contribution gives larger errors for higher tubes.

6 Beam divergency and attenuation

From distributions like ones shown in fig.2-6 we estimated divergency of both X-ray beams. In fig.13 dependence of sigma gaussian fit for the wire shadow in counting rate as a function of relative distance of wire along beam direction is shown. Zero distance corresponds to the lowest layer of tubes (tubes 1-4 in fig. 1). Divergency of the 1st beam is about $2.8 \cdot 10^{-4}$ and about $1.8 \cdot 10^{-4}$ for the 2nd one.

Mean counting rate for the beam near center of a tube as a function of Al thickness is shown in fig.14. Thickness of glue was not taken into account. It was detected that there are two samples of tube with about 0.5 mm wall thickness which have about of 10% difference of beam attenuation. Measured wall thickness is different for these samples by about of 30μm.

7 Some X-ray voltage dependences

We measured the wire position in tube 1 by the beam 2 at different anode voltages of X-ray tube. Fig.15 shows dependences of counting rate versus Al thickness for X-ray high

voltage from 18 to 26 kV with step 1 kV. Glue and gas layer was not taken into account. Measurement were done at tube high voltage 2.2 kV.

Fit error of wire 1 coordinate versus X-ray high voltage is given in fig.16 when the wire was measured by different drift tubes. Digits near curves indicate tube number where the 1st tube wire shadow was measured.

8 Conclusion

1. We have the two-beam X-ray pulser. Both beams have width quite enough for measurement of 50 μm tungsten wires inside MDT tubes.
2. The pulser is placed on hand-driven platform which can be moved at distance 1m relative position of which can be measured with 5 μm step.
3. At X-ray tube anode voltage 23 kV we could be able to measure wires in 4 layers of tubes using the tubes as detector of X-ray.
4. Errors of wire position from fit of the counting rate deep is 1 μm for the 1st layer, 2-6 μm for the 2nd layer, 7-14 μm for the 3d layer and 15-25 μm for the 4th layer for U_{X-ray}=23 kV.
5. Fit wire position errors versus tube layer and high voltage of X-ray pulser are measured for one of the X-ray beam.
6. Temporal stability gives RMS error 17 μm for the 1st layer wire.
7. Temperature variation is about 20-25 μm/°C.
8. One wire measurement requires about 15 minutes after preliminary estimation of wire position.
9. Tube wall of the 1st layer can be measured in direction normal to the beams with precision about 10-20 μm.
10. Results of the 4x8 drift tube prototype measurements by X-ray are follow (all indicated errors are RMS):
    (a) difference between predicted wire position and measured one is:
        i. for X-coordinate 13±21 μm;
        ii. for Y-coordinate -1±33 μm;
        iii. normal to beam 1 5±32 μm;
        iv. normal to beam 2 9±33 μm;
    (b) outer tube diameter is 29.970±50 μm;
    (c) difference between predicted wall position and measured one is -5±75 μm;
    (d) Measured displacement of wire with respect to wall is 1±60 μm.

References

1. A.Borisov et al, ATLAS Internal Note, Muon-No-059, 24 November 1994.

2. A.Borisov et al, ATLAS Internal Note, Muon-No-069, 26 January 1994.

3. L.Vertogradov, ATLAS Internal Note, Muon-No-041, June 1994. L.vertogradov, presentation to Vienna Wire Chamber Conference,1995.

4. N.I.Bozhko et al., In Pros. of the 3d Workshop on IHEP-JINR Neutrino Detector, JINR, P1,2,13-83-81, 1983, p.30.

5. Yu.B.Bushnin et al, Preprint IHEP 82-141.

Tables

TABLE 1. Difference between predicted and measured wire coordinate.

Tube number	1	2	3	4	5	6	7	10
$X_{predicted}$-$X_{measured}$, μm	36	22	0	-38	38	19	2	26
$Y_{predicted}$-$Y_{measured}$, μm	-50	-18	0	-22	-30	16	10	11
Tube number	11	12	13	14	15	22	27	
$X_{predicted}$-$X_{measured}$, μm	16	22	-1	7	48	-4	2	
$Y_{predicted}$-$Y_{measured}$, μm	28	0	-37	59	65	100	-34	

TABLE 2.1 Difference between predicted and measured wire position normal to beam 1.

Tube number	1	2	3	4	5	6	7	8
$P_{predicted}$-$P_{measured}$, μm	58	28	0	22	49	9	2	-16
Tube number	10	11	12	13	14	15	16	19
$P_{predicted}$-$P_{measured}$, μm	17	0	-18	16	22	-10	-69	3
Tube number	20	22	23	24	27	28	32	
$P_{predicted}$-$P_{measured}$, μm	1	53	28	0	-18	10	-69	

TABLE 2.2 Difference between predicted and measured wire position normal to beam 2.

Tube number	1	2	3	4	5	6	7	9
$P_{predicted}$-$P_{measured}$, μm	5	10	0	44	17	25	8	-6
Tube number	10	11	12	13	14	15	17	18
$P_{predicted}$-$P_{measured}$, μm	28	29	19	-20	36	75	-73	1
Tube number	21	22	25	26	27			
$P_{predicted}$-$P_{measured}$, μm	-52	47	-103	-11	15			

TABLE 3. Outer tube diameter (mm) normal to beam.

Tube number	1	2	3	4	16	24
Measured by beam 1	30.007	29.943	29.947	30.042		
Measured by beam 2	30.037	29.883	29.939	29.978	30.075	29.984

Figure captions

1. Setup for X-ray tomography of the prototype.
2. Wire in tube 1 measured by X-ray 1 in tubes 1,5,10,14,19,23.
3. Wire in tube 5 measured by X-ray 1 in tubes 10,14,19,23
4. Wire in tube 10 measured by X-ray 1 in tubes 14,19,23.
5. Wire in tube 14 measured by X-ray 1 in tubes 19,23.
6. Wire in tube 16 measured by X-ray 2 in tubes 16,20,23,27,30.
7. Distribution of differences between predicted and measured wire coordinates: a) for X-coordinate; b) for Y-coordinate; c) in direction normal to beam 1; d) in direction normal to beam 2.
8. Counting rate dependences for tubes 1,2,5,9 when width range covering tube 1 was scanned by X-ray beam 2.
9. Dependences of counting rate of tubes 1,5,9 when X-ray beam 2 crosses wall of tubes 1 and 5.
10. Distributions of difference between: 30 mm and measured outer diameter of tube (a); predicted wall position and measured one (b); difference between ideal and measured wire-to-wall distance (c).
11. Long period measurements of wire in tube 4 by the X-ray beam 1: a) measured position of the wire as a function of time; b) measured position of the wire as a function of temperature of the table; c) distribution of measured wire position corresponding to a) and b); d) distribution of the measured wire position with temperature cut 20.7°C.
12. Long period measurements of wire in tube 1 by the X-ray beam 2: a) measured position of the wire as a function of time; b) measured position of the wire as a function of temperature of the table; c) distribution of measured wire position corresponding to a) and b); d) distribution of the measured wire position with temperature cut 20.3°C.
13. Dependence of wire shadow width as a function of relative distance along beam.
14. Beam attenuation as a function of Al thickness.
15. The 2nd beam attenuation measured in tubes 1,5,10,14,19,28,32 for X-ray high voltage from 18 to 26 kV. Tube voltage 2.2 kV.
16. The 1st tube wire fit error versus X-ray high voltage measured in different tubes.

09/12/95 12.41

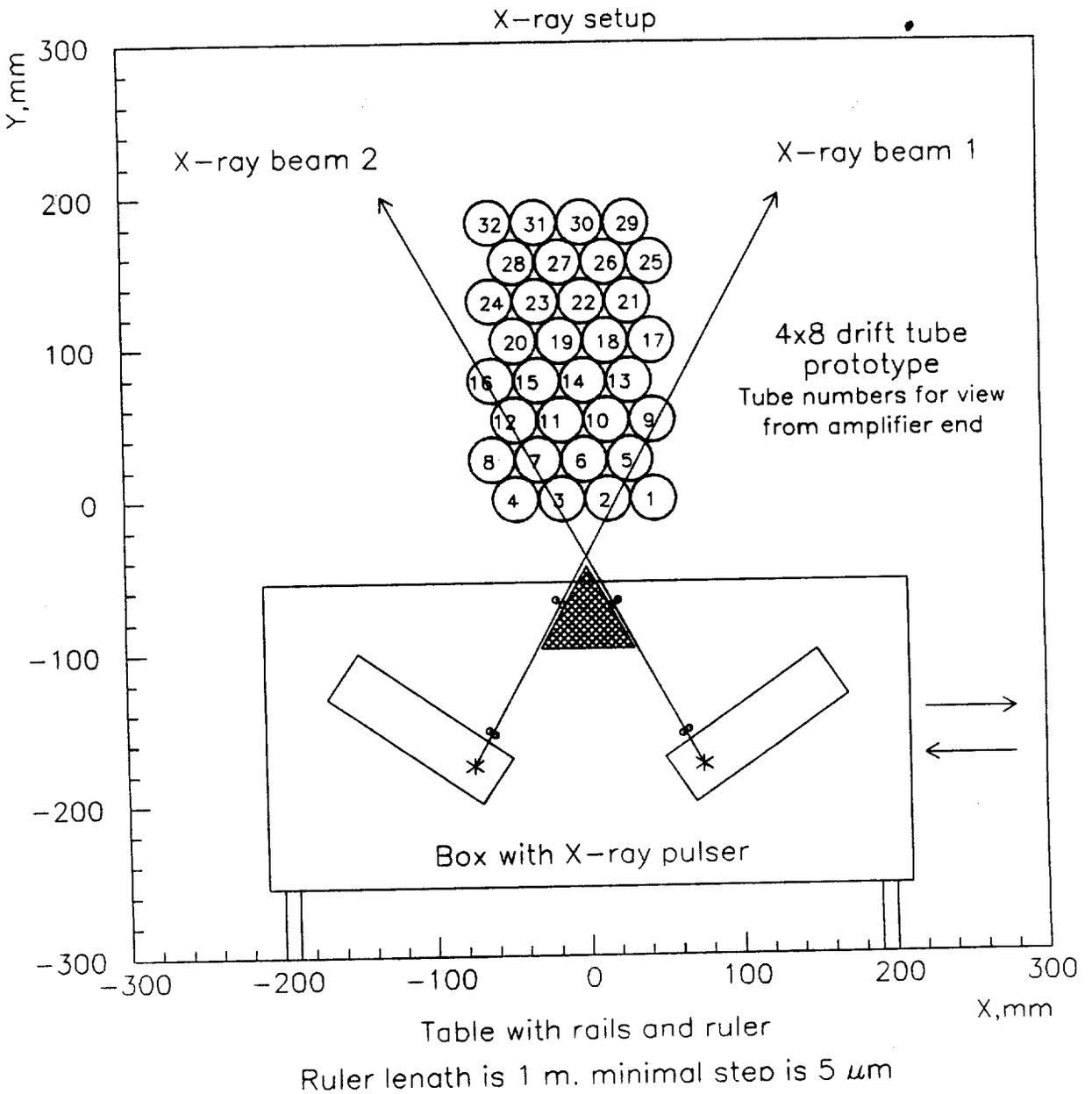

Fig. 1

15/11/95 09.05

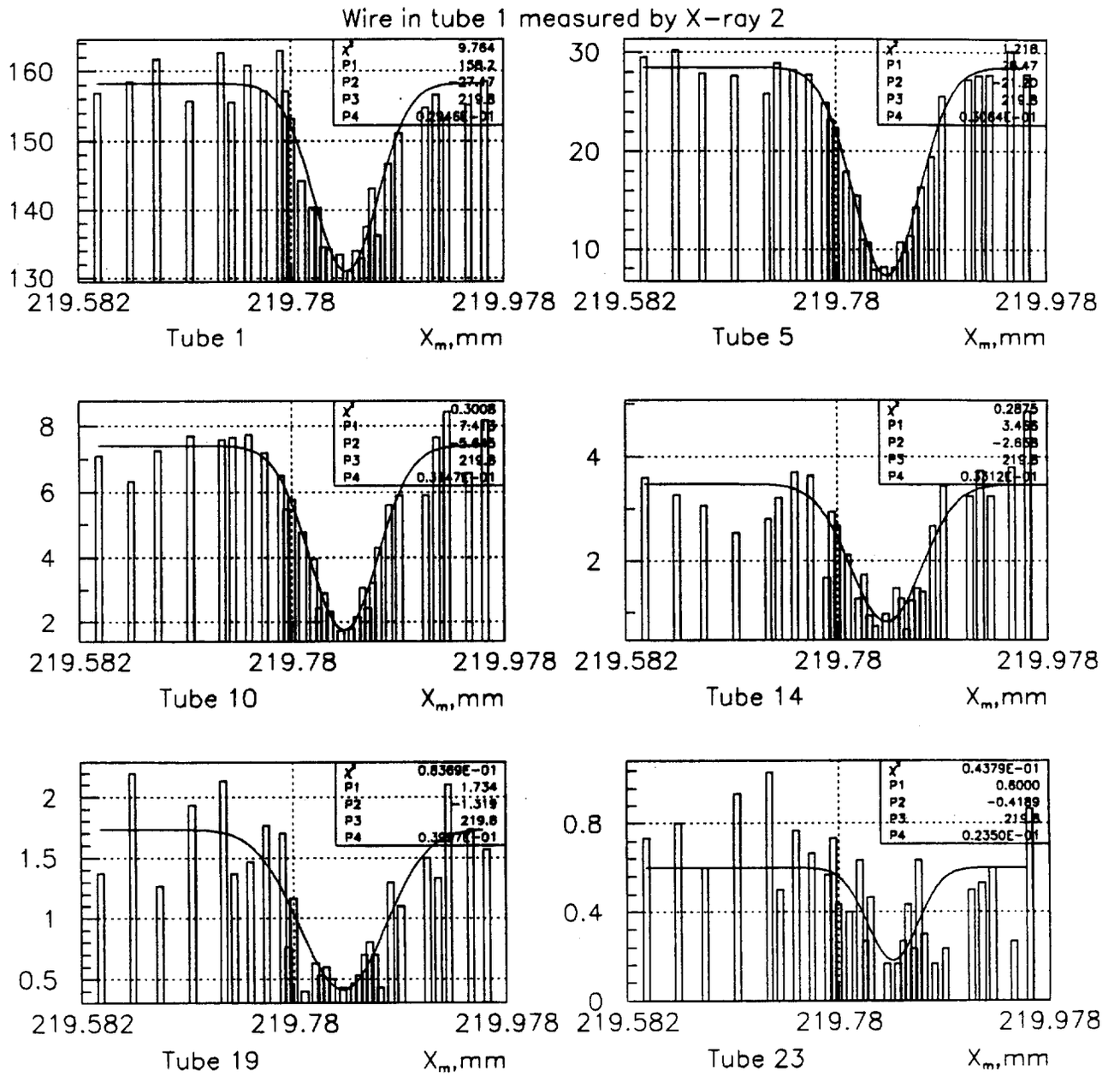

Fig 2.

15/11/95 09.20

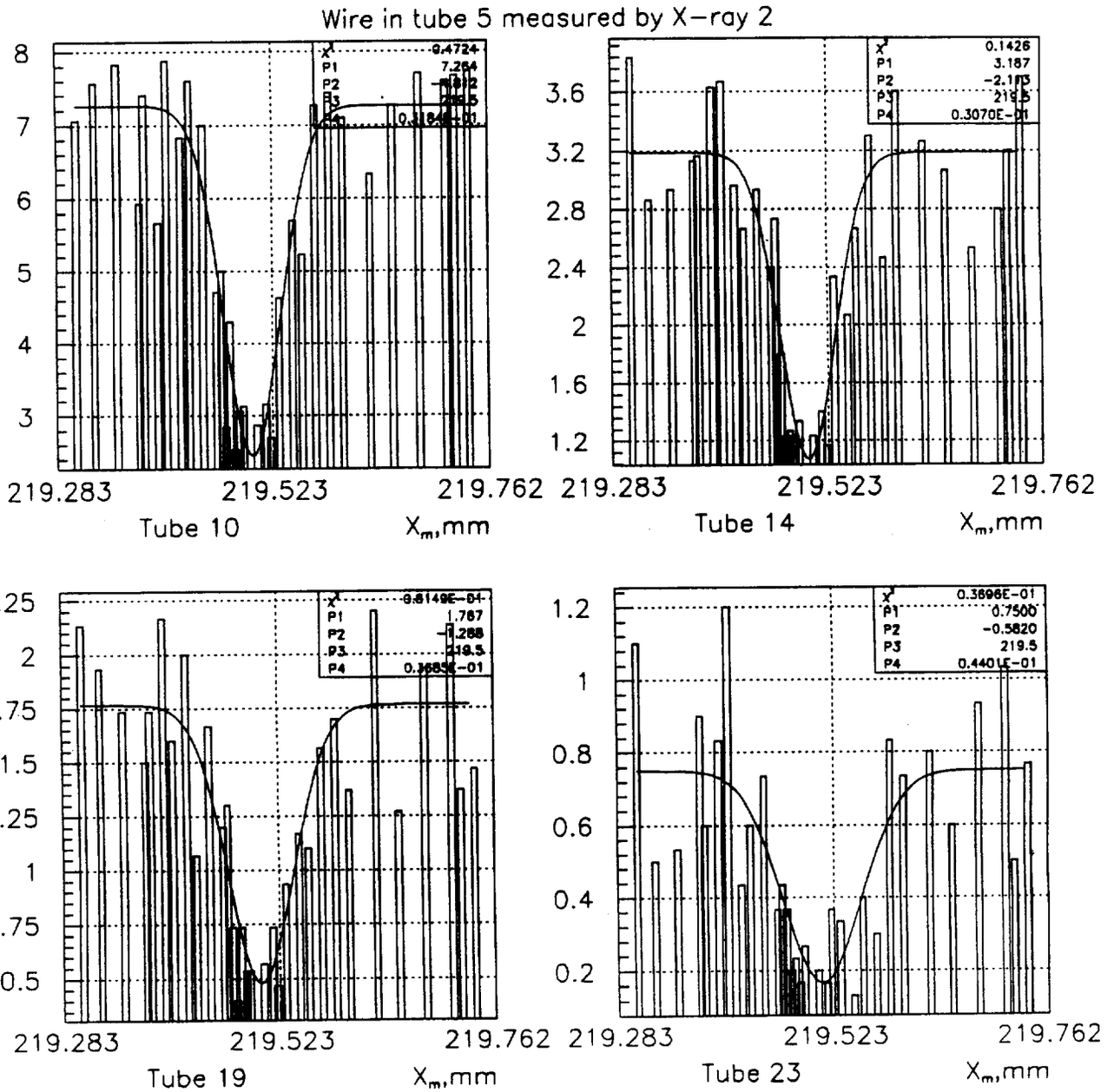

Fig 3

15/11/95 09.35

Wire in tube 10 measured by X−ray 2

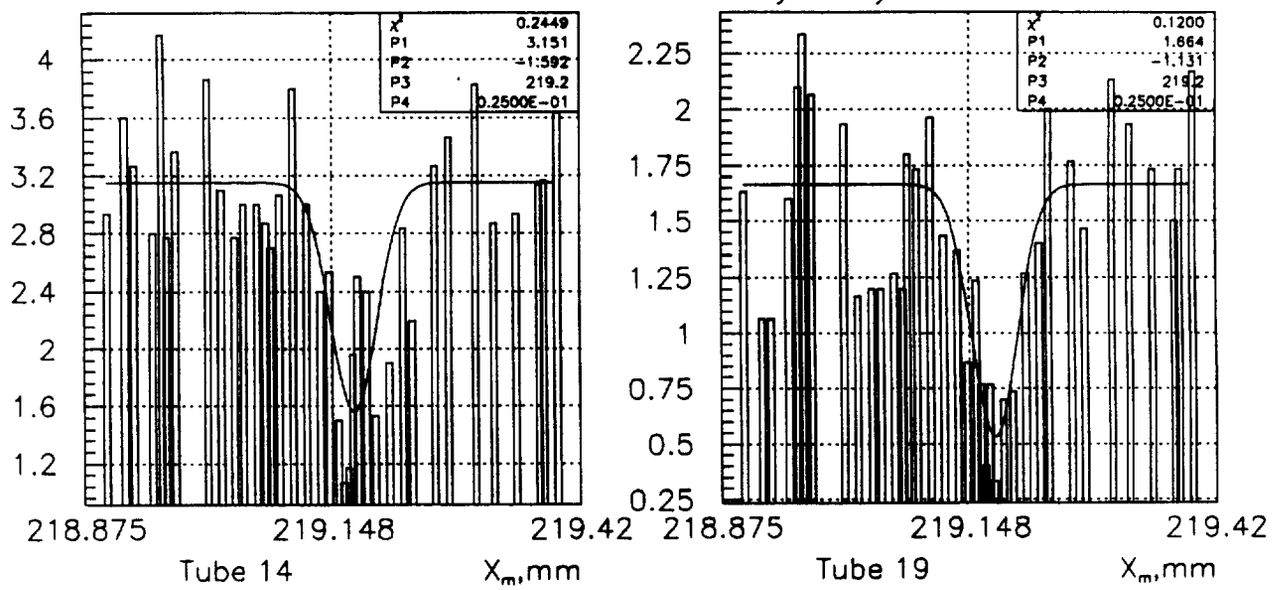

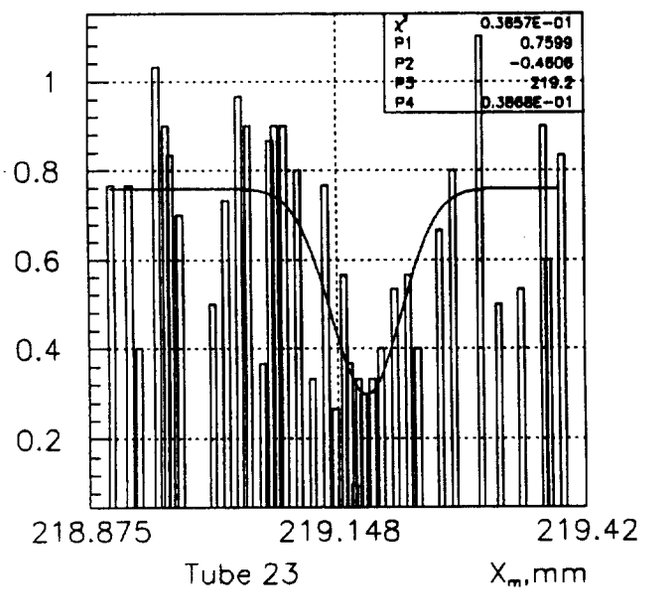

Fig 4

15/11/95 10.11

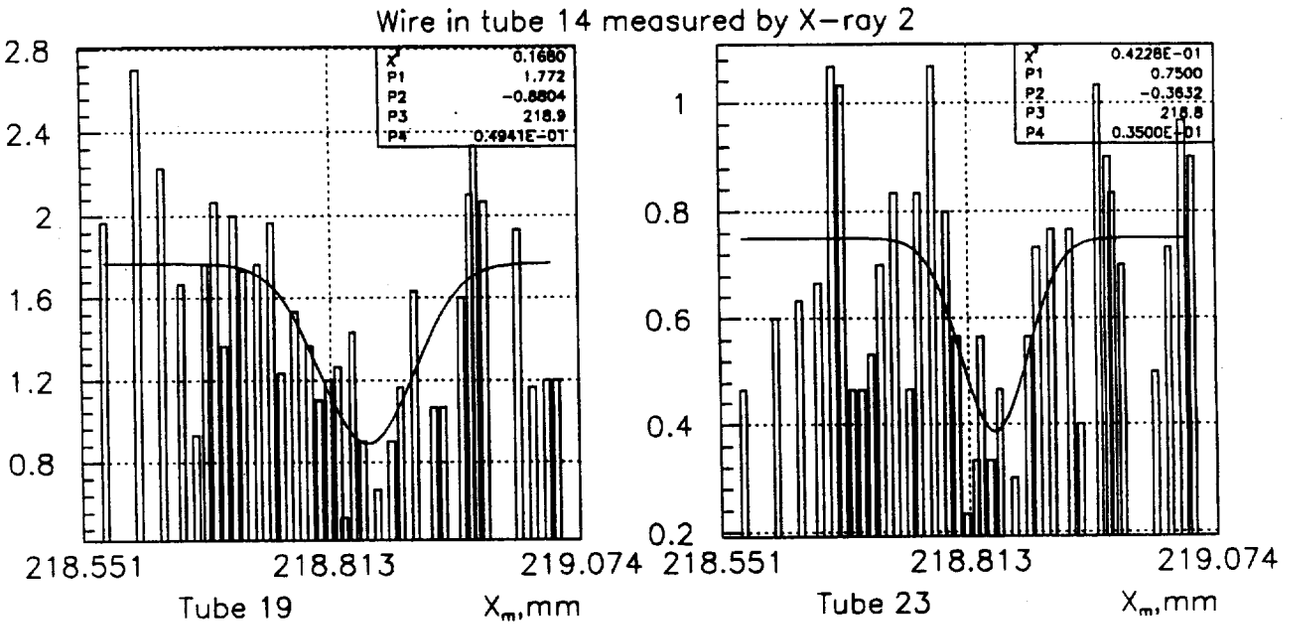

Fig. 5

16/11/95 17.22

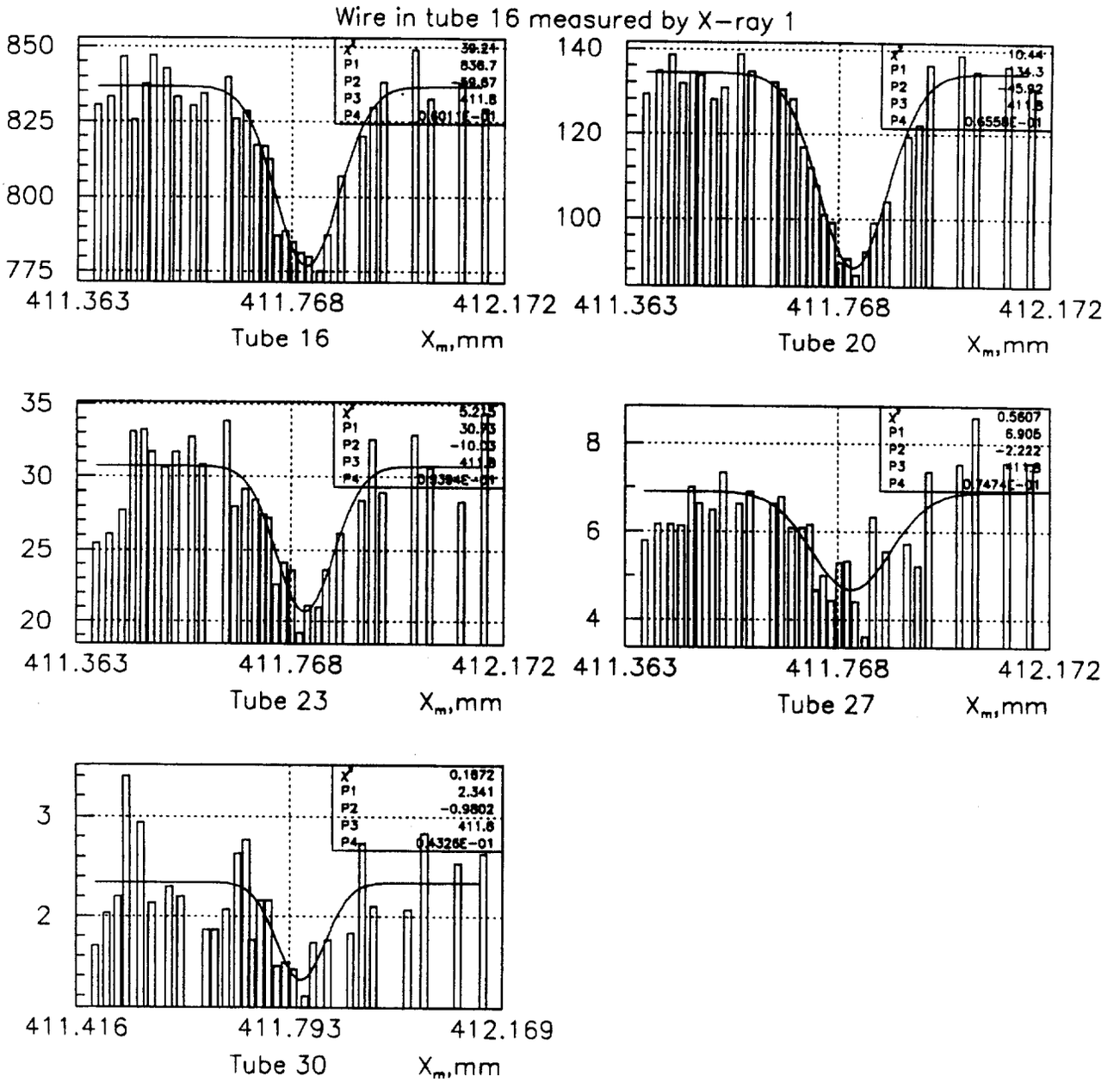

Fig. 6

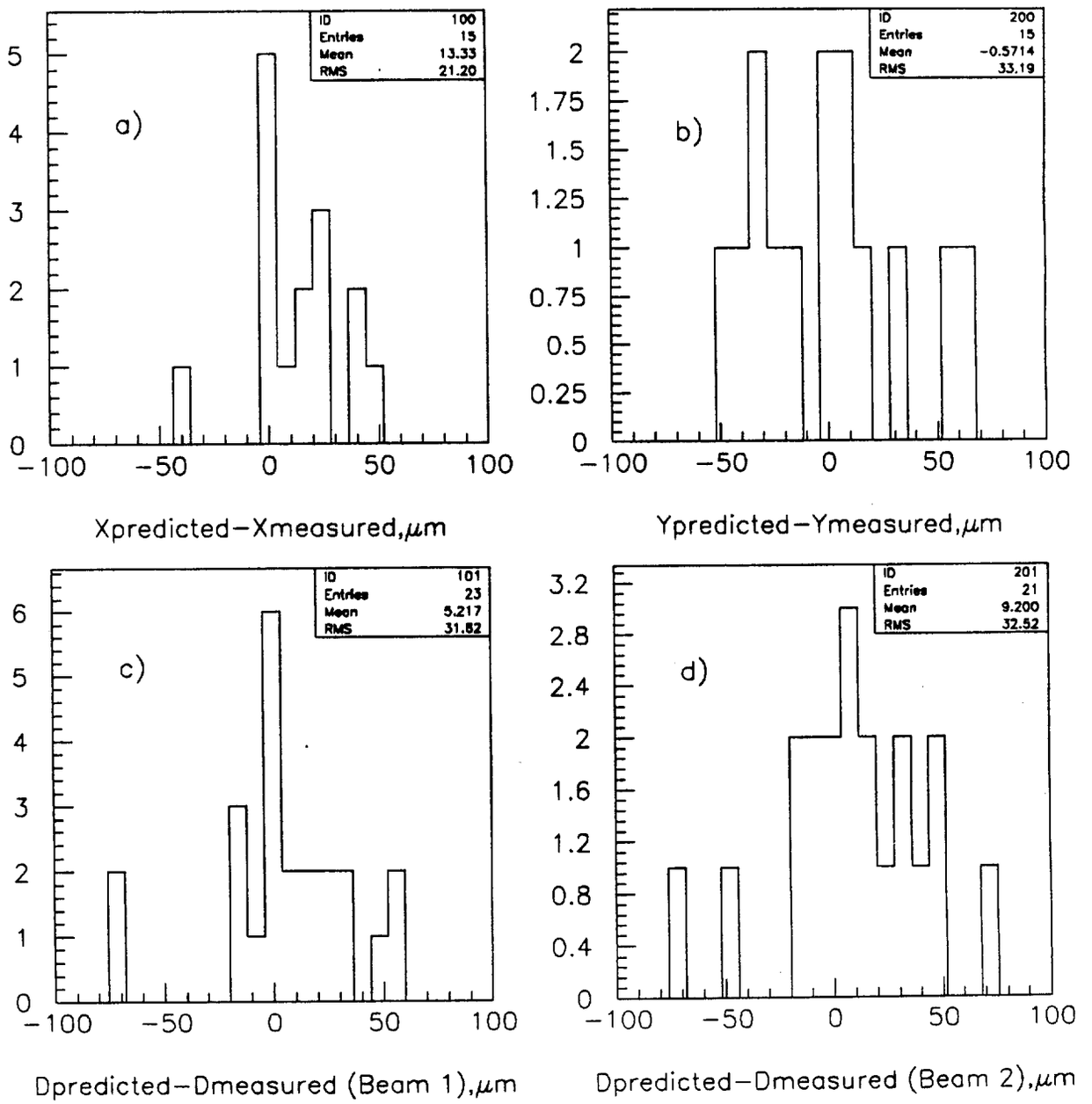
ID 100
Entries 15
Mean 13.33
RMS 21.20
a)
Xpredicted−Xmeasured,μm
ID 200
Entries 15
Mean −0.5714
RMS 33.19
b)
Ypredicted−Ymeasured,μm
ID 101
Entries 23
Mean 5.217
RMS 31.82
c)
Dpredicted−Dmeasured (Beam 1),μm
ID 201
Entries 21
Mean 9.200
RMS 32.52
d)
Dpredicted−Dmeasured (Beam 2),μm

Fig. 7

30/11/95 09.32

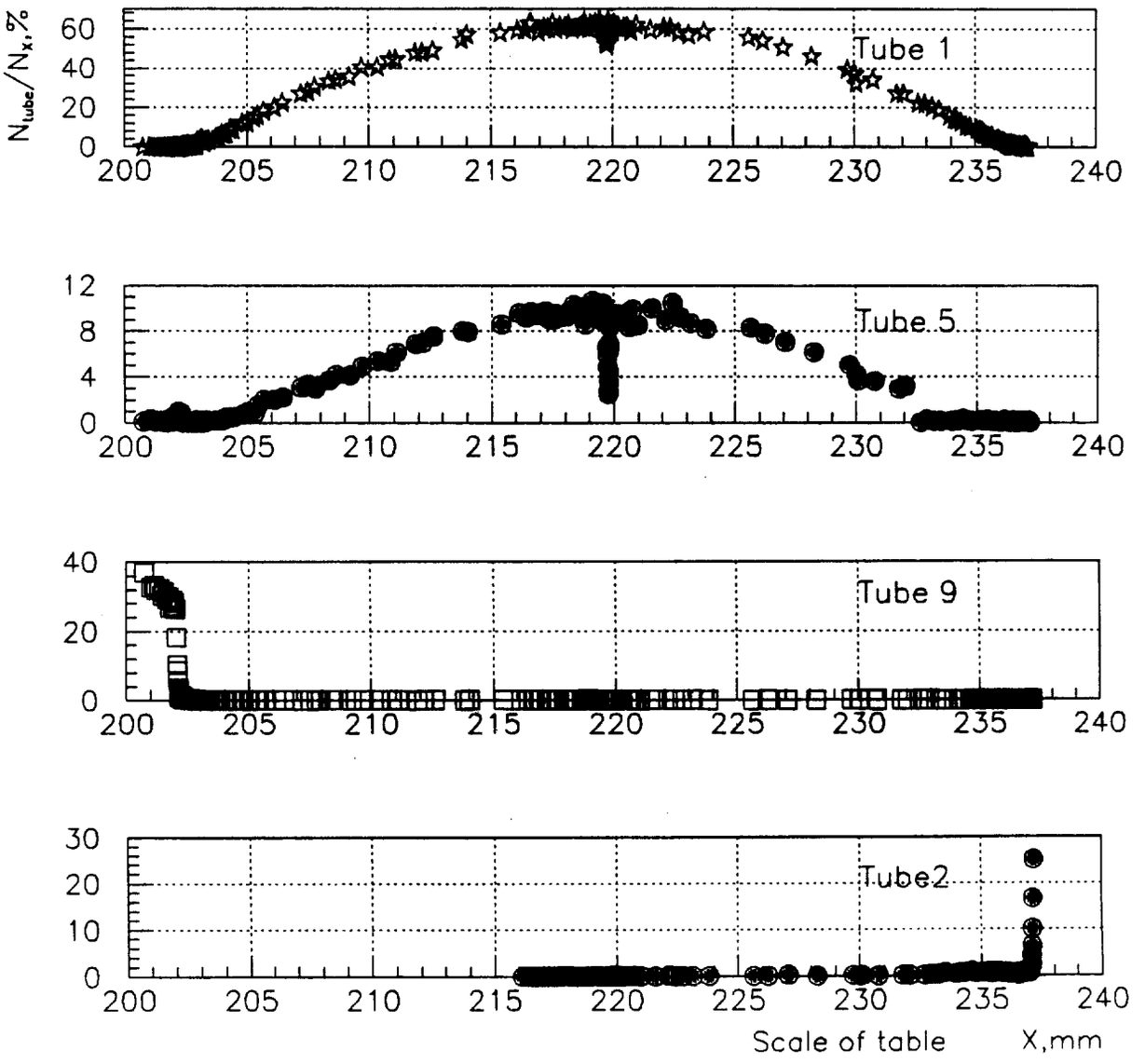

Fig. 8

01/12/95 08.51

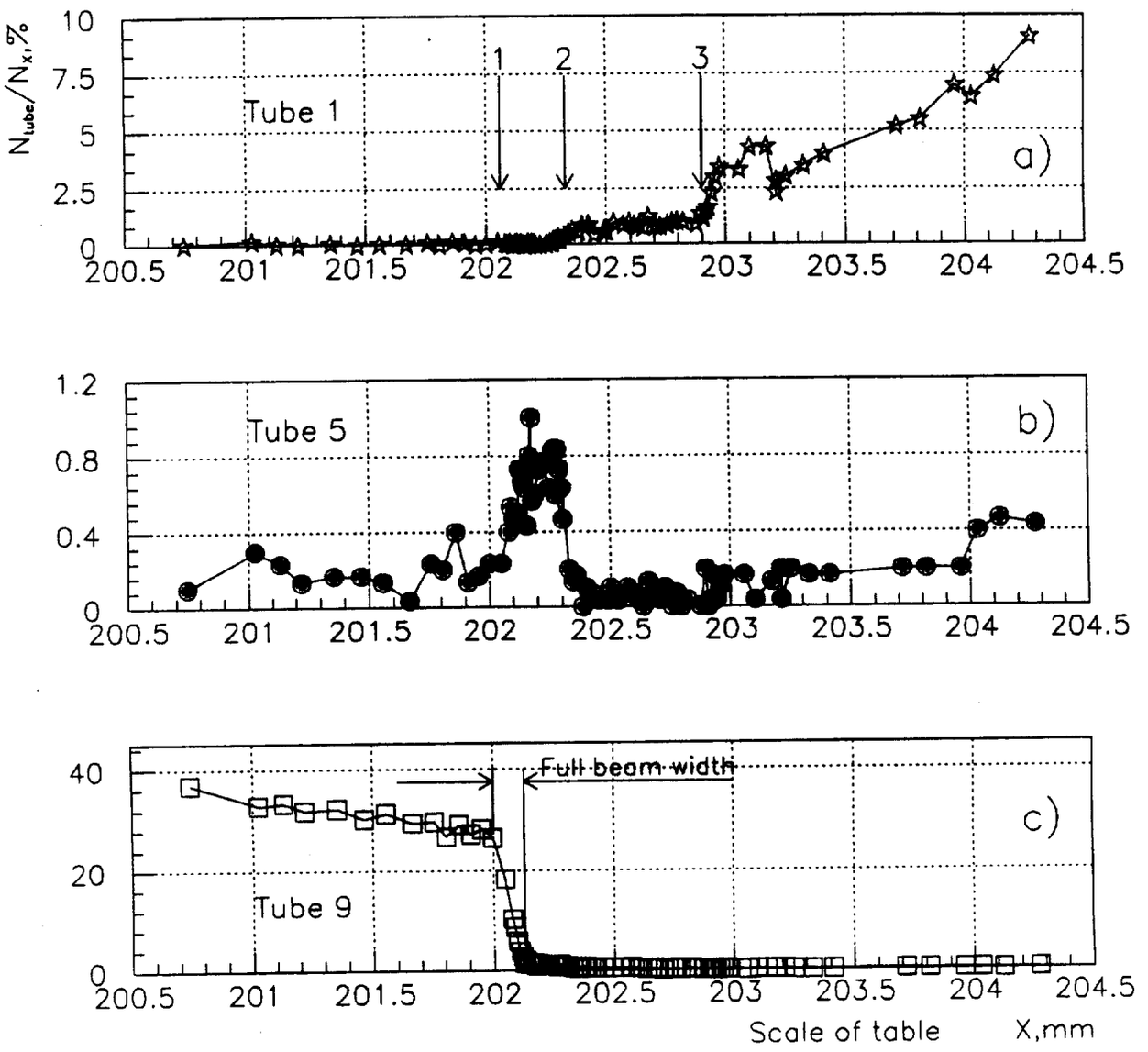

Fig. 9

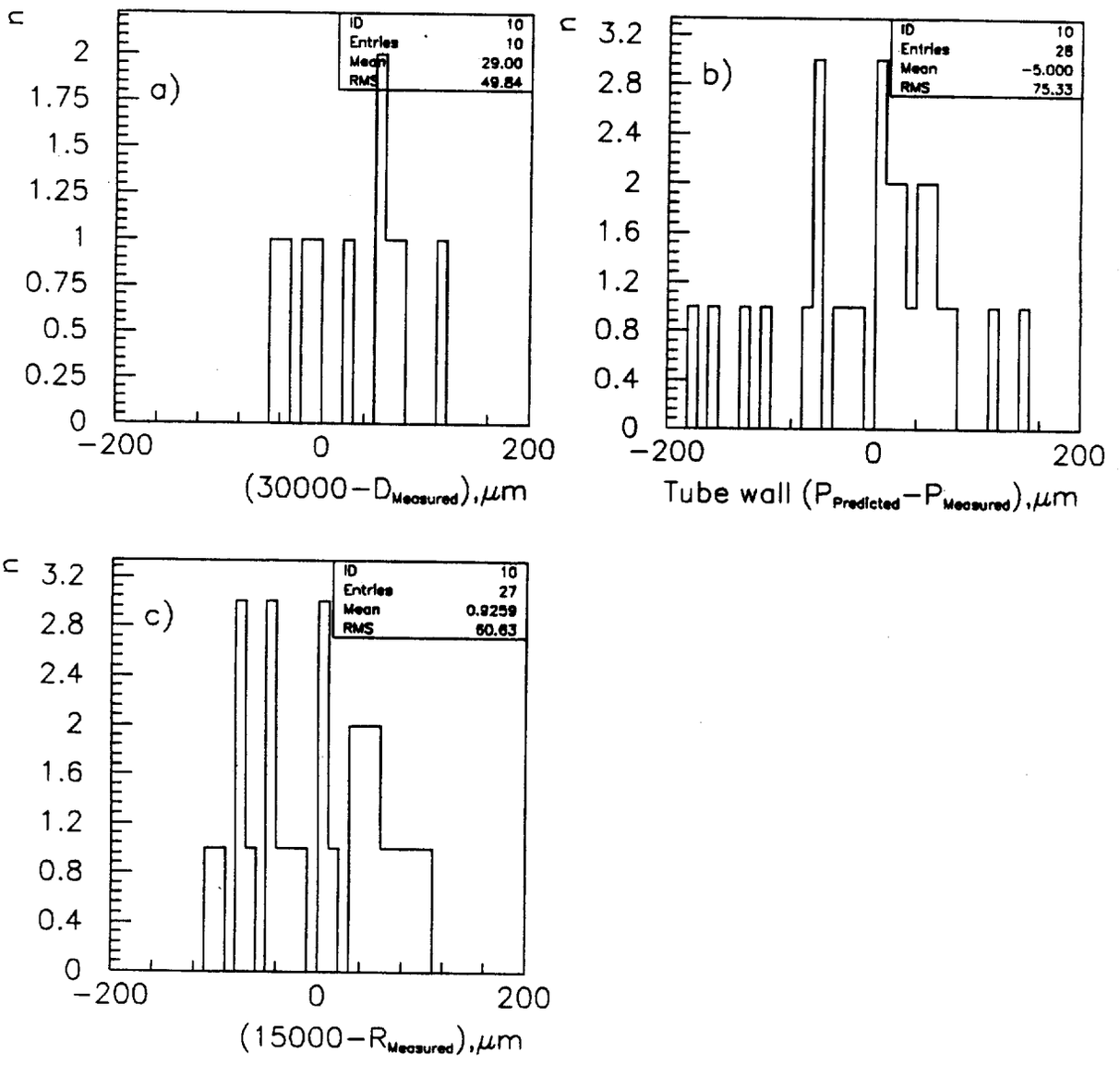
n
a)
ID 10
Entries 10
Mean 29.00
RMS 49.84
2
1.75
1.5
1.25
1
0.75
0.5
0.25
0
−200
0
200
(30000−D Measured), μm
n
b)
ID 10
Entries 28
Mean −5.000
RMS 75.33
3.2
2.8
2.4
2
1.6
1.2
0.8
0.4
0
−200
0
200
Tube wall (P Predicted − P Measured), μm
n
c)
ID 10
Entries 27
Mean 0.9259
RMS 60.63
3.2
2.8
2.4
2
1.6
1.2
0.8
0.4
0
−200
0
200
(15000−R Measured), μm

Fig. 10

06/12/95 14.53

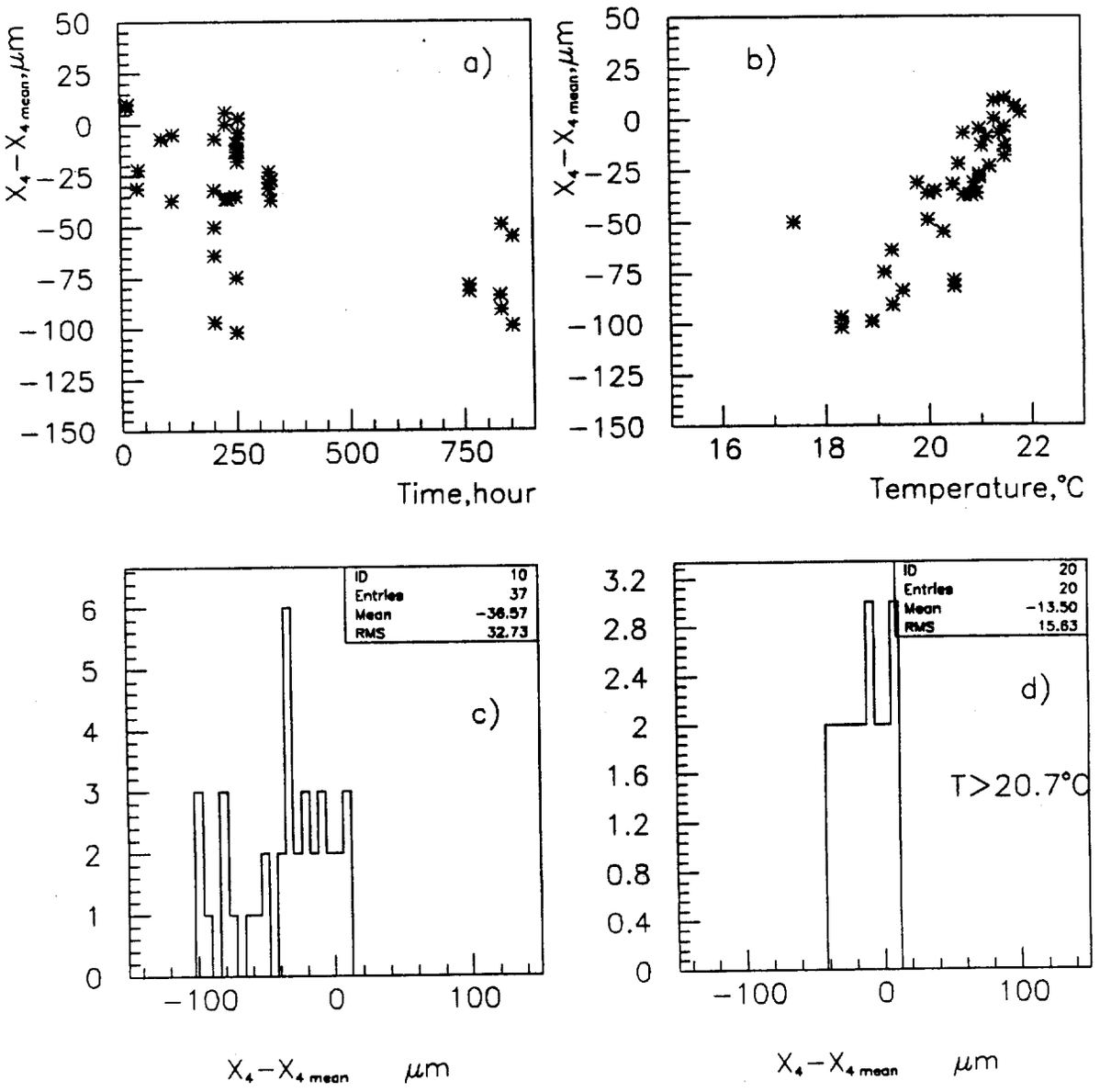

Fig.11

06/12/95 14.33

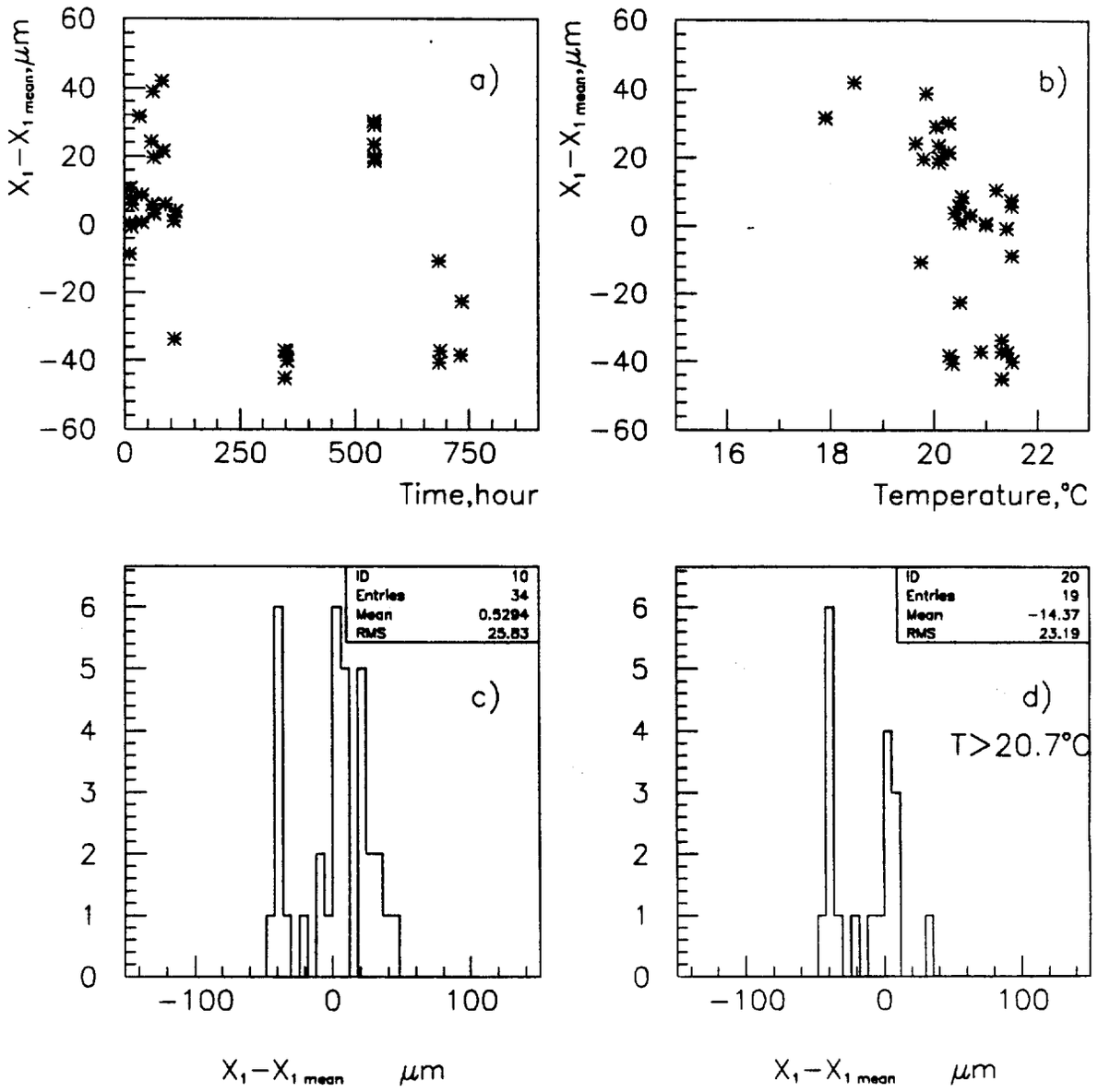

Fig. 12

22/11/95 09.20

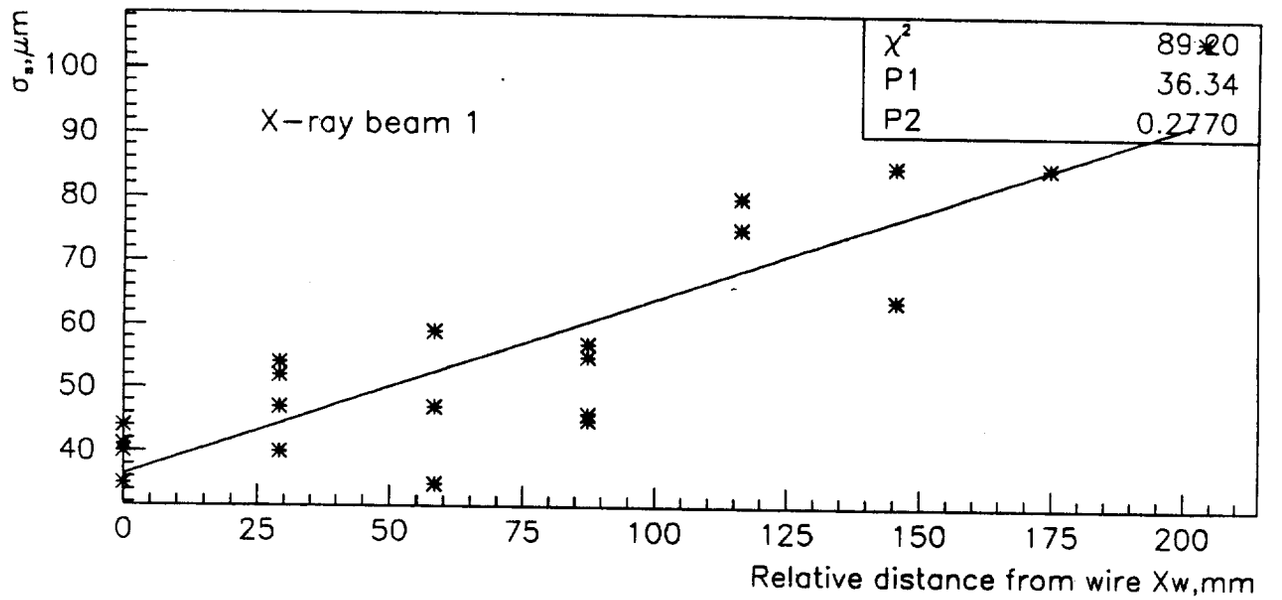

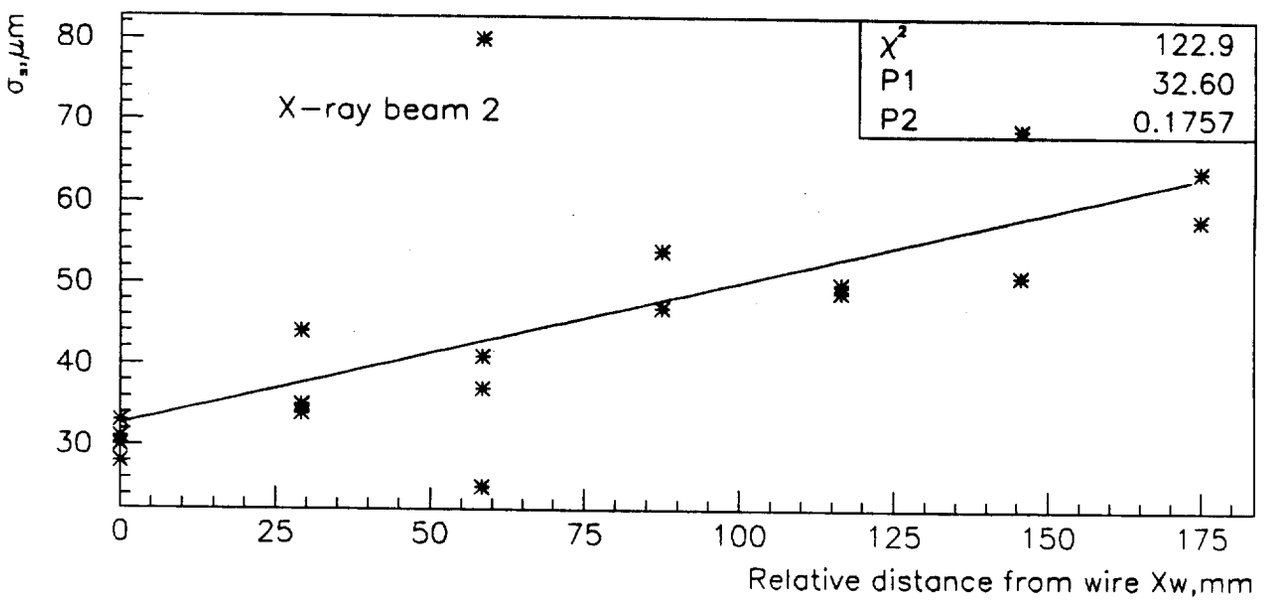

Fig.13

23/11/95 11.59

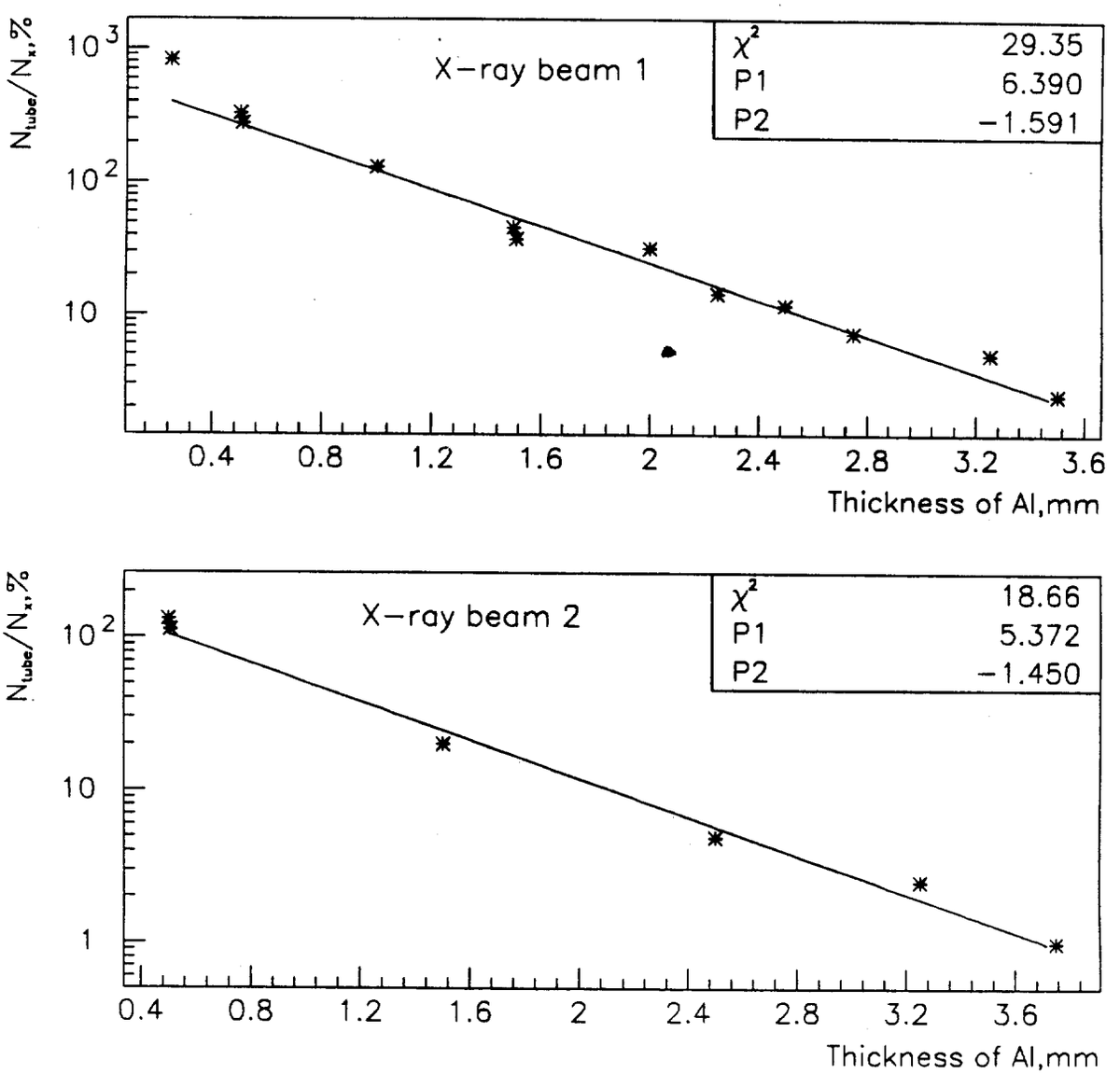

Fig. 14

23/11/95 11.56

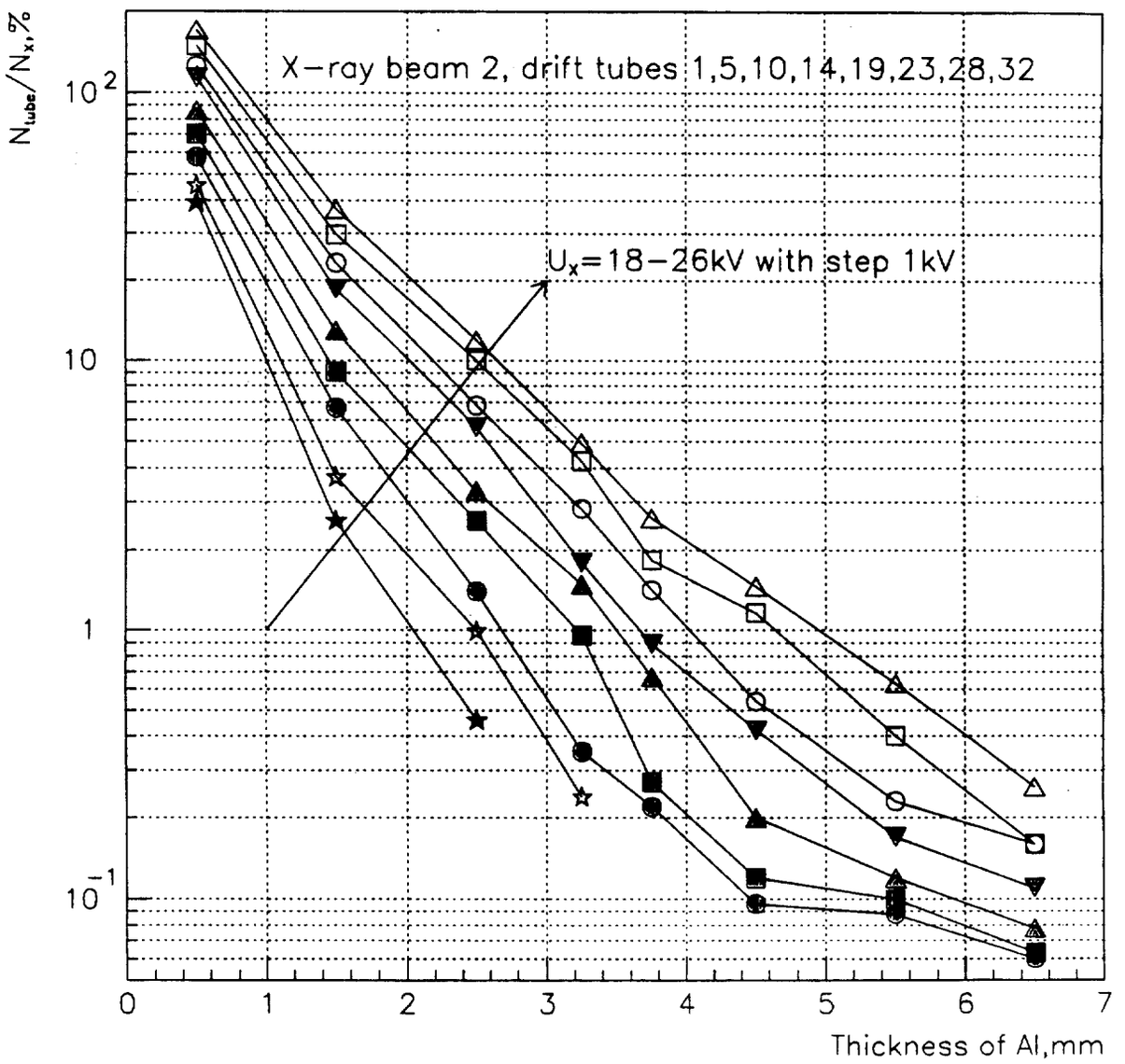

Fig. 15

23/11/95 11.53

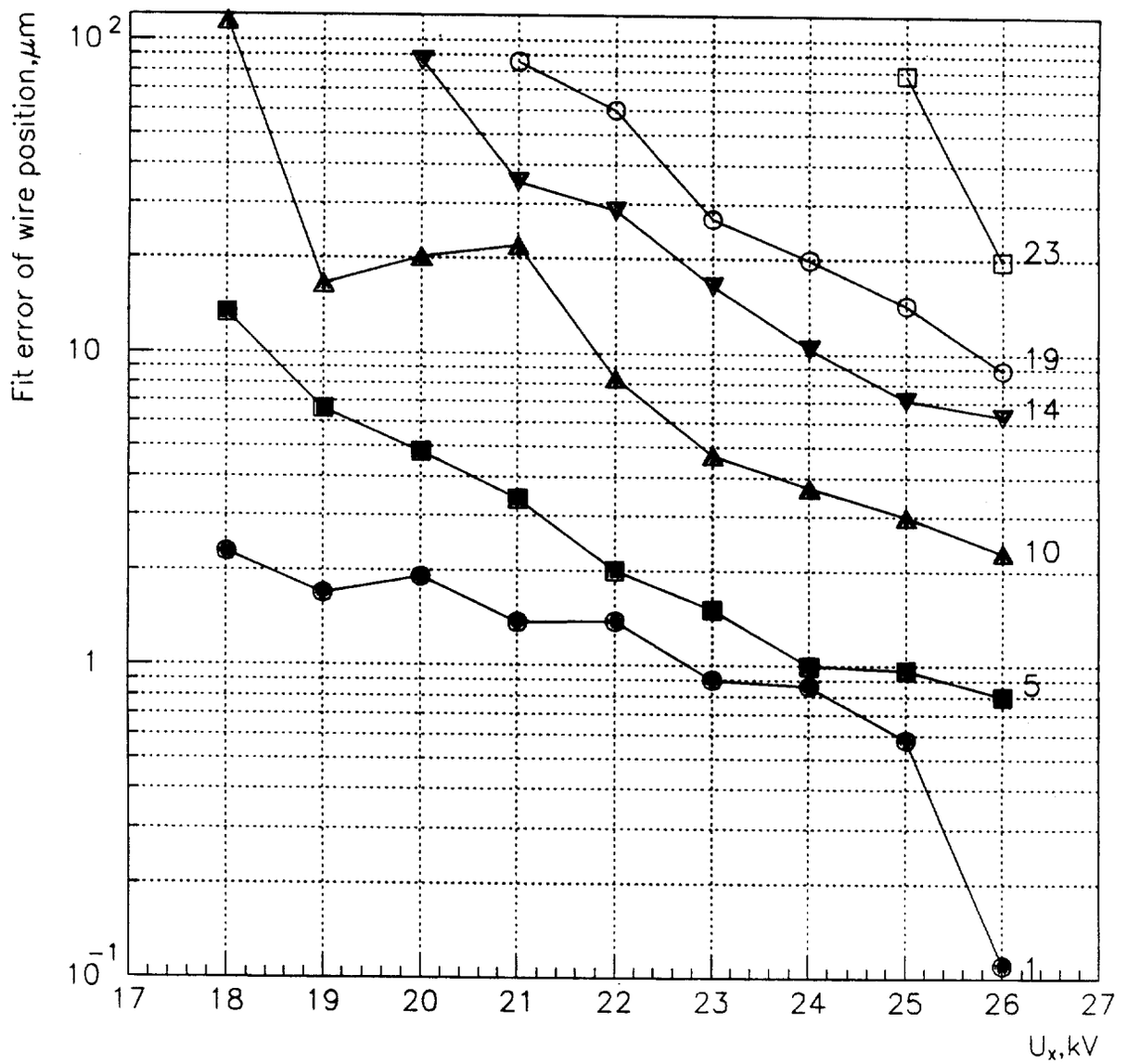

Fig 16

13/02/96 17.00

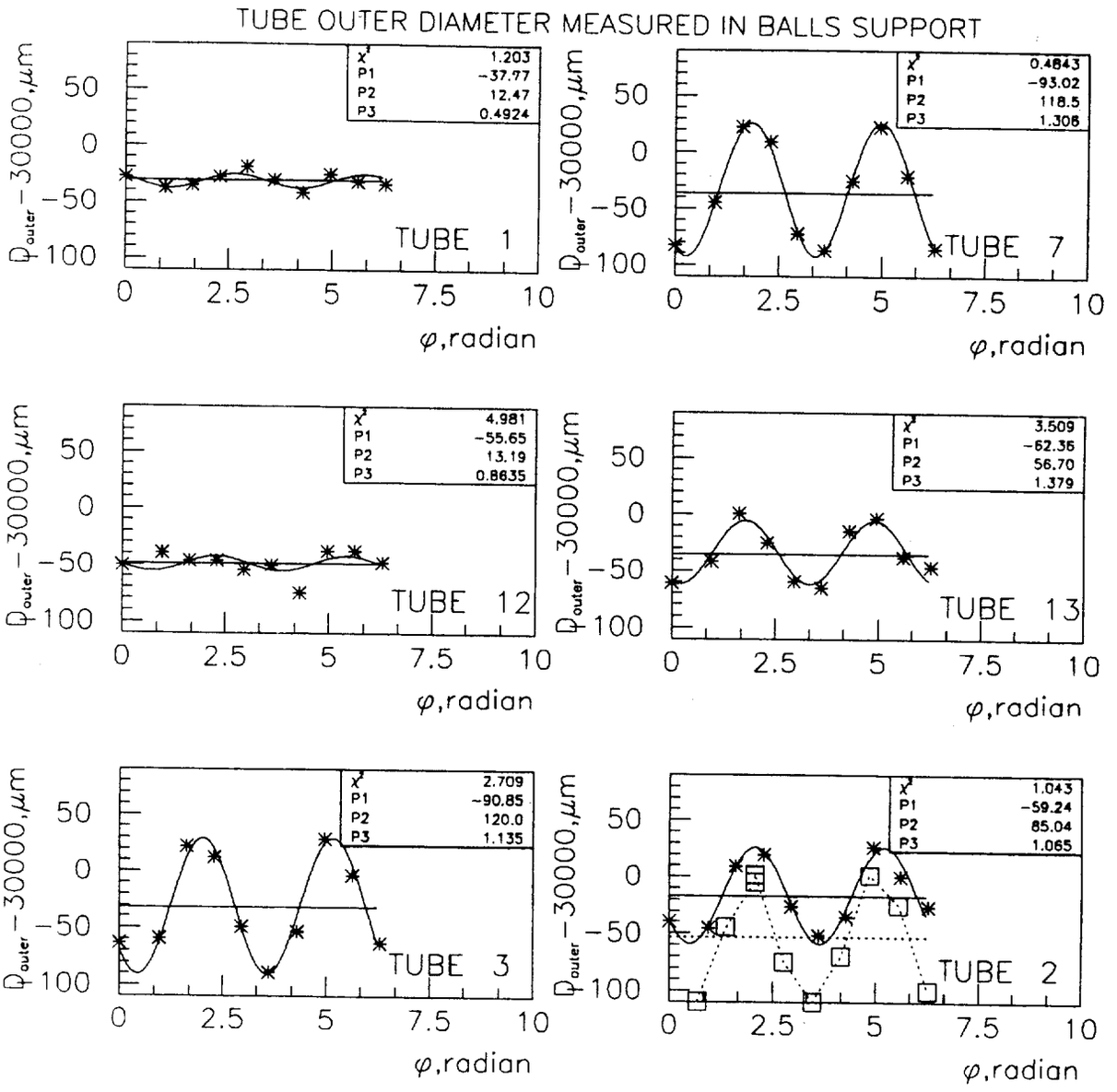

Fig 8